Pharm Res (2012) 29:2264–2275
DOI 10.1007/s11095-012-0754-0

RESEARCH PAPER

Identification and Characterization of a Novel Class of Atypical Dopamine Receptor Agonists

E. V. Kuzhikandathil • S. Kortagere

Received: 24 January 2012 / Accepted: 11 April 2012 / Published online: 1 May 2012

ABSTRACT

Purpose The D3 dopamine receptor exhibits tolerance and slow response termination (SRT) properties that are not exhibited by the closely-related D2 dopamine receptor. We previously demonstrated that the induction of tolerance elicits a unique conformational change in the D3 receptor. Here we tested the hypothesis that the tolerance and SRT properties of the D3 receptor are ligand-dependent.

Methods We used pharmacophore modeling and *in silico* screening approaches coupled with electrophysiological and biochemical methods to identify and functionally characterize the novel dopamine receptor agonists.

Results We identified cis-8-OH-PBZI (PBZI), FAUC73 and an additional novel compound, ES609, which although they are full D3 receptor agonists, do not induce the tolerance and SRT properties of the D3 receptor. In addition, PBZI has full intrinsic activity at D2L, is a partial agonist at D2S and exhibits functional selectivity at D4.2 dopamine receptors. ES609 is a partial agonist at D2S, D2L and D4.2 receptors, and exhibits functional selectivity at D2L and D4.2 dopamine receptors.

Conclusion We have discovered a novel class of atypical dopamine receptor agonists that include three structurally dissimilar compounds. These new agonists will help determine the physiological and pathophysiological relevance of D3 receptor tolerance and SRT properties.

KEY WORDS dyskinesia · Parkinson's disease · pharmacophore modeling · receptor conformation · signal transduction

ABBREVIATIONS

cAMP	cyclic adenosine monophosphate
EC	extracellular
EC_{50}	half-maximal effective concentration
GIRK	G protein–coupled inward rectifier potassium
GPCR	G protein–coupled receptor
hERG	human ether-à-go-go related gene
HSB	hybrid structure–based
IBMX	3-isobutyl-1-methylxanthine
IC	intracellular
MAP	mitogen-activated protein
MD	molecular dynamics
OPLS	optimized potentials for liquid simulations
PBZI	cis-8-hydroxy-3-(n-propyl)-1,2,3a,4,5,9b-hexahydro-1H-benz[e]indole hydrobromide
POPC	1-palmitoyl-2-oleoyl-sn-glycero-3-phosphocholine
RMSD	root mean square deviation
SRT	slow response termination
TM	transmembrane
β_2-AR	β_2-adrenergic receptor

INTRODUCTION

The neurotransmitter dopamine controls a wide variety of physiological and behavioral functions in mammals via five major subtypes of dopamine receptors. They are broadly classified as "D1-like" and "D2-like" dopamine receptors based on pharmacology and function. The D1-like receptors include D_1 and D_5 receptors, and D2-like receptors include D_2, D_3, and D_4 receptors. The D_3 receptor primarily couples to the pertussis toxin-sensitive Gα-proteins (Gi/Go) (1). When transfected into different cell lines, the D_3 receptor couples to the adenylate cyclase V isoform (2) and initiates

Electronic supplementary material The online version of this article (doi:10.1007/s11095-012-0754-0) contains supplementary material, which is available to authorized users.

E. V. Kuzhikandathil (✉)
Department of Pharmacology & Physiology,
UMDNJ-New Jersey Medical School
MSB, I-647, 185 South Orange Avenue
Newark, New Jersey 07103, USA
e-mail: kuzhikev@umdnj.edu

S. Kortagere
Department of Microbiology and Immunology, Drexel University
College of Medicine
Philadelphia, Pennsylvania 19129, USA

signaling events including phosphorylation of mitogen-activated protein (MAP) kinases (3,4). D_2 and D_3 dopamine receptors also modulate potassium and calcium channel function (5,6). We have shown that transfected D_3 receptors couple robustly to natively expressed G protein-coupled inward rectifier potassium (GIRK) and voltage-gated P/Q type calcium channels and inhibit firing of spontaneous action potentials and secretory activity in the AtT-20 neuroendocrine cell line (7–9). We have also shown that the D_3 receptor couples to natively expressed adenylate cyclase V (10), MAP kinases (4) and ion channels (11) in AtT-20 cells.

We have previously reported that the D_3 dopamine receptor exhibits tolerance and slow response termination (SRT) properties that distinguish it from the closely related D_2 dopamine receptors (11). The tolerance property of the D_3 receptor is the progressive decrease in receptor signaling function upon repeated stimulation by classical agonists, including dopamine. The SRT property is the prolongation of time taken to terminate the signaling function of the D_3 receptor, after removal of the agonist. The D_3 receptor tolerance property is distinct from classical desensitization as it develops only after the removal of agonist; there is negligible loss of response in the continued presence of agonists. We have also shown that the tolerance property is not mediated by D_3 receptor internalization, persistent agonist binding or a change in binding affinity (4,11). We have hypothesized that tolerance and SRT properties provide functionally distinguishable roles for D_3 and D_2 dopamine receptors, resulting in differential modulation of *in vivo* neuronal activity and locomotor behaviors (4). Our structure-function studies have identified the structural features of the D_3 receptor that determine these two properties (4,11). Mutating the C147 residue in the second cytoplasmic loop of the D_3 receptor to a positively charged amino acid residue, results in a mutant D_3 receptor that exhibits SRT but not the tolerance property (4).

Our recent study demonstrated that agonist-induced tolerance in D_3 receptors is associated with a unique conformational state of the receptor (12). The association of tolerance with a unique conformation state led us to hypothesize that the tolerance and SRT properties of the D_3 receptor are ligand dependent and that agonists that altered the tolerance-specific conformation would not induce the tolerance and SRT properties. Here we tested this hypothesis by screening known D_3 receptor agonists and determining their ability to induce the tolerance and SRT properties. We identified two existing agonists, cis-8-OH-PBZI (PBZI) and FAUC 73, which although they are full agonists at D_3 receptors, failed to induce its tolerance and SRT properties. We developed a pharmacophore model based on the interactions of PBZI with the D_3 receptor as an input to the hybrid structure-based (HSB) *in silico* screening method (13) and identified an additional novel agonist, ES609, which also did not induce D_3 receptor tolerance and SRT properties. Using electrophysiological and biochemical approaches we characterized the functional properties of this new class of atypical D_3 dopamine receptor agonists. In the context of D_3 receptor signal transduction, our studies have identified a novel class of agonists that modulate specific receptor signaling properties, pharmacologically converting the D_3 receptor to the functional equivalent of a D_2 receptor with respect to activation of GIRK channels and modulation of action potential firing. Interestingly, these agonists also exhibited functional selectivity at the D_2 and $D_{4.2}$ dopamine receptor subtypes and showed differential efficacy for activating signaling pathways coupled to the D_{2S} and D_{2L} dopamine receptor splice isoforms.

MATERIALS AND METHODS

Computational Modeling (HSB Method)

The HSB protocol for designing small molecule inhibitors to GPCRs has been described in detail by Kortagere and Welsh (13). Briefly, the method involves creating a focused library of small molecules derived from commercial vendors. All molecules in the database were converted to the UNITY format and screened using UNITY module integrated in SYBYL (SYBYL 8.0, Tripos International). At the time the project was initiated, the recently reported *antagonist*-bound crystal structure of D_3 receptor (14) was not available and hence the entire screening was performed using a homology model of D_3 receptor. To create a three-dimensional pharmacophore based on the interactions of PBZI in the D_3 receptor binding site, a homology model of the D3 receptor was created using the crystal structure of the β_2-adrenergic (β_2-AR) receptor in complex with a partial inverse agonist (PDB code: 2RH1) as a template (15). We used the homology modeling program Modeller (ver 9.4) (16) as previously described (12,17). PBZI has a fairly rigid conformation owing to its tricyclic structure. Similarly, FAUC73 has a di-propyl group extending from the amine group. To obtain the best conformation of these alkyl tail regions extending from the amine group, we performed a conformational analysis using the stochastic search method adopted in Molecular Operating Environment (MOE; Chemical Computing Group, Montreal, Quebec, Canada). All conformations obtained were clustered based on energy and a representative member from the most populated cluster was chosen for further optimization using the AM1 semi-empirical quantum chemical method adopted in MOE. A similar procedure was used for other ligands in this study. The optimized conformations were used for further docking experiments. Previous studies have shown that the amine groups of known D_3 receptor ligands form a salt bridge with Asp110 of the D_3 receptor. To facilitate this interaction, the amine groups of all the ligands were set to a

protonated state. PBZI and FAUC73 were docked to the three-dimensional structure of the refined D_3 structure using the docking program GOLD ver 4.1 (Genetic Optimisation for Ligand Docking; Cambridge Crystallographic Data Centre [CCDC], Cambridge, UK) (18). Twenty independent runs were performed to adequately sample the ligand and receptor conformational space. The docked complexes were scored using Goldscore (18), Chemscore (19) and the customized scoring scheme described previously (13). To obtain a more realistic conformation of the agonist-bound model, the D_3-PBZI complex was immersed in an explicit water-POPC lipid bilayer-water model membrane system using the Desmond module (20) of the Schrodinger suite program. The model membrane was prealigned to the β_2-AR crystal structure to adopt its orientation to our D_3 receptor-PBZI model. Default conditions for bilayer composition including those of Na^+ and Cl^- ions were chosen and the entire simulation was performed using the default all-atom OPLS (optimized potentials for liquid simulations) force field (47). To completely refine the model, we carried out a production run of 3 ns and followed a four-step protocol that included routines for prerelaxation, minimization, heating, and equilibration (14). Throughout the simulations, the interactions of PBZI with residues from transmembrane 3 and transmembrane 5 (TM3 and TM5) were maintained using low levels of constraints. However, all constraints were removed during the production run to completely relax the ligand in the protein environment. Key interactions between PBZI and the D_3 receptor, namely the salt bridge with Asp110, the hydrogen bond interaction with Ser192, the aromatic ring interactions with His349, and the hydrophobic interactions with Val111 and other aromatic residues from TM6 were used to build a four-point hybrid pharmacophore as shown in Fig. 6b. Electronic libraries of vendor-available small molecules were screened to identify hits that corresponded to the pharmacophore. Finally, the hits were filtered using Lipinski's rule of 5 (21), blood–brain barrier (BBB) penetration (22) and off-target screening against pregnane xenobiotic receptors (23) and human ether-à-go-go related gene (hERG) channels (24). The resulting 290 hits were docked to the binding site of the D_3 receptor using the GOLD program and scored using a variety of scoring functions as described previously for docking of PBZI. The 15 best-ranking hits were obtained from the vendors and functionally evaluated.

Cell Culture

AtT-20 mouse pituitary cells were grown in Ham's F10 medium with 5 % fetal bovine serum, 10 % heat-inactivated horse serum, 2 mM glutamine and 50 μg/mL gentamicin (Invitrogen, Carlsbad, CA, USA). AtT-20 cells stably expressing the human D_{2S}, D_{2L}, D_3, and $D_{4.2}$ receptors were maintained in the above F10 culture media supplemented with 500 μg/mL G418 (Invitrogen). For electrophysiological characterization, cells were plated onto glass coverslips coated with 40 μg/mL poly L-lysine (Sigma, St. Louis, MO, USA). The generation and characterization of the AtT-20 cells stably expressing various human dopamine receptors have been previously reported (8,10).

Drugs and Solutions

(4aR-Trans)-4,4a,5,6,7,8,8a,9-octahydro-5-propyl-1 H-pyrazolo[3,4-g]quinoline hydrochloride (Quinpirole; Sigma); R-(+)-trans-3,4,4a,10b-tetrahydro-4-propyl-2 H,5 H-(1)benzopyrano[4,3-b]-1,4-oxazine-9-ol (PD128907; Tocris, Ellisville, MO, USA); (+)-7-hydroxy-2-aminopropylaminotetralin (7OH-DPAT; Tocris); (S)-2-amino-4,5,6,7-tetrahydro-6-(propylamino)benzothiazole dihydrochloride (pramipexole; Tocris); (6 S)-5,6,7,8-tetrahydro-6-[propyl[2-(2-thienyl)ethyl] amino]-1-naphthalenol hydrochloride (rotigotine; Tocris); 4-(2-chlorophenyl)-butan-2-amine (ES609; Asinex, Winston Salem, NC, USA); and cis-8-hydroxy-3-(n-propyl)-1,2,3a,4,5,9b-hexahydro-1 H-benz[e]indole hydrobromide (PBZI; Sigma) were dissolved in water and used at indicated concentrations. (R)-(−)-2-[5-(4-fluorophenyl)-3-pyridylmethylaminomethyl]-chromane hydrochloride (sarizotan; Merck KGaA, Darmstadt, Germany); [4-Ethynylcyclohex-3-enyl] dipropylamine (FAUC73; Sigma); and (RS)-trans-7-Hydroxy-2-[N-propyl-N-(3′-iodo-2′-propenyl)amino]tetralin maleate (7OH-PIPAT; Tocris) were dissolved in DMSO. A 10 mM stock of dopamine (Sigma) was freshly dissolved in 100 mM ascorbic acid and used at a final concentration of 100 nM. Figure 1 shows the chemical structures of dopamine, PBZI, ES609, PD128907, FAUC73 and quinpirole.

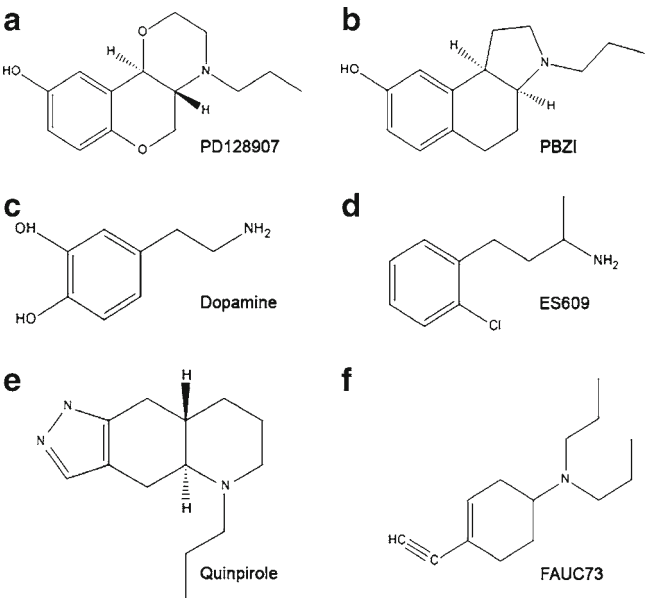

Fig. 1 Chemical structures of the ligands discussed in the study. (**a**) PD128907, (**b**) PBZI, (**c**) dopamine, (**d**) ES609, (**e**) quinpirole, and (**f**) FAUC73.

Measurement of cAMP

Cyclic adenosine monophosphate (cAMP) levels were assessed using the cAMP Biotrak Enzymeimmunoassay (EIA) kit (GE Healthcare, Piscataway, NJ, USA) as described previously (10). The cAMP levels in each treated sample were assayed in triplicate and the entire experiment was repeated three independent times.

Electrophysiology

Agonist-activated currents were measured by the whole-cell patch clamp technique in voltage clamp and current clamp mode as described previously (7,8,10). Drug solutions were delivered to cells via a multi-barreled micropipette array. The current responses are normalized to the cell capacitance, to account for variation in cell size.

Statistics

Analysis of variance (ANOVA) and the Holm-Sidak multiple pair-wise comparison tests and Student *t*-test were performed with the SigmaPlot® 11 software (SPSS Inc., Chicago, IL, USA). Data were considered statistically significant when P was less than 0.05.

RESULTS

D_3 Receptor Tolerance and SRT Properties are Ligand Dependent

Figure 2 shows the D_3 dopamine receptor-induced activation of native GIRK channels when the receptor is stimulated with the endogenous agonist dopamine. The tolerance property of D_3 receptor is quantified as the ratio of second to first agonist-induced response. We have previously shown that the D_3 receptor tolerance property is also observed in the D_3 receptor-adenylate cyclase and -MAP kinase pathways (4). In addition, Fig. 2 shows the D_3 receptor SRT property, which is the delayed termination of the agonist-induced response after agonist removal. In a previous study, we showed that tolerant D_3 receptor adopts a distinct conformation (12), suggesting that tolerance and SRT properties might be modulated by agonists that alter this distinct conformational state. To identify agonists that might modulate D_3 receptor tolerance and SRT properties, we screened 10 different agonists for their ability to induce tolerance and SRT using the D_3 receptor-GIRK channel signaling pathway as an assay. The selected agonists included the endogenous ligand dopamine, ligands that exhibited selectivity for D_3, and compounds used to treat Parkinson's disease in the clinic. The results in Fig. 3 show that although

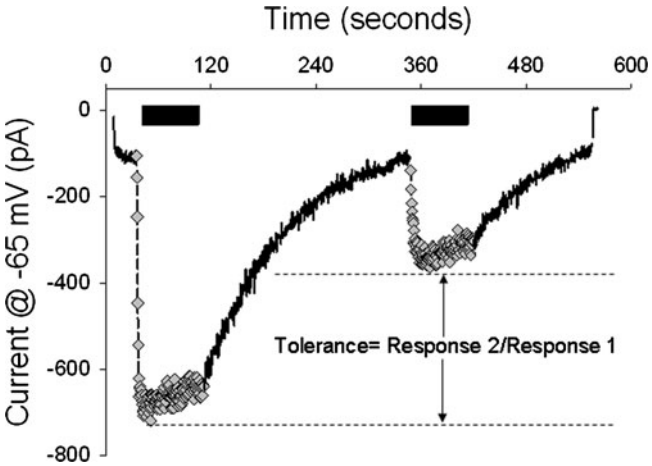

Fig. 2 Dopamine-induced tolerance and SRT properties are exhibited in cells expressing the D_3 dopamine receptor. Representative voltage clamp recording from an AtT-20 cell stably expressing the human D_3 dopamine receptor. The cell was held at −65 mV and inward currents elicited by 100 nM dopamine (gray diamonds/black bar) dissolved in extracellular solution with 30 mM potassium (to enhance GIRK currents). Tolerance is quantified as the ratio of second to first response. The duration of agonist application was ~60 s.

most agonists induced tolerance, two agonists, PBZI and FAUC73, did not induce the tolerance property. Interestingly, PD128907 induced enhanced tolerance that was significantly different from the other agonists. Figure 4 shows representative voltage clamp recordings of AtT-20 cells stably expressing the human D_3 dopamine receptor and

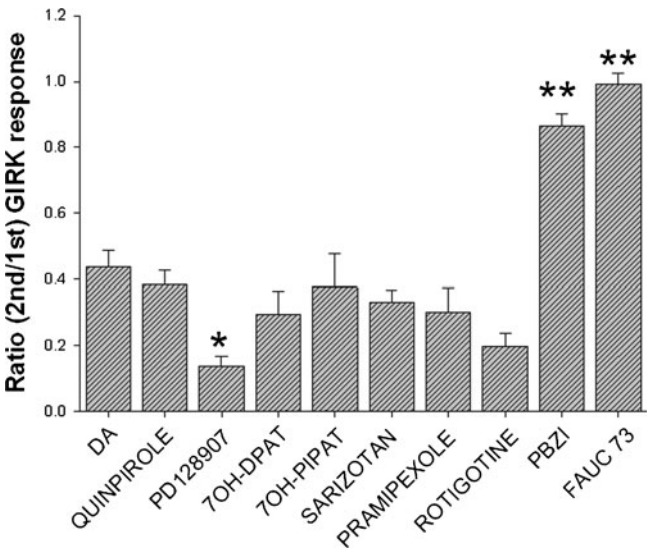

Fig. 3 The tolerance property of D_3 receptor is agonist-dependent. Cumulative data show the ratio of second to first agonist-induced GIRK response in AtT-20 cells stably expressing the human D_3 dopamine receptor. GIRK responses were elicited using dopamine (DA, 100 nM, n=5), quinpirole (100 nM, n=5), PD128907 (100 nM, n=5), 7OH-DPAT (100 nM, n=4), 7OH-PIPAT (100 nM, n=4), sarizotan (100 nM, N=6), pramipexole (300 nM, n=4), rotigotine (100 nM, n=4), PBZI (300 nM, n=10), and FAUC 73 (300 nM, n=4). Error bars represent ± SEM. *, **, $P<0.05$, ANOVA, *post-hoc* Holm-Sidak test.

treated with agonists that either induce tolerance or do not induce tolerance. PBZI (Fig. 4a) and FAUC73 (Fig. 4b) did not induce tolerance and SRT properties; however in the same cell, quinpirole (Fig. 4a) and PD128907 (Fig. 4b) induced severe tolerance and SRT. Control experiments in parental AtT-20 cells, as well as pretreatment with the D_2/D_3 receptor antagonist, eticlopride (100 nM), showed that the agonistic effects of PBZI and FAUC73 are specific for D_3 receptors (Supplementary Material Fig. S1A and B). Furthermore, the inability to induce tolerance and SRT was not concentration dependent; PBZI tested at doses from 100 nM to 10 μM did not induce tolerance (Supplementary Material Fig. S1C). Together, these results suggest that the D_3 receptor tolerance and SRT properties are ligand dependent. Of the two compounds, PBZI is water soluble and has been more extensively characterized *in vitro* and *in vivo* (25–27); therefore, its structure was used to identify additional D_3 receptor agonists in subsequent studies.

D_3 Receptor Signaling Properties Affect Cellular Function and Signaling Pathways

We have previously shown that the stably expressed D_3 receptor couples to endogenous GIRK channels in AtT-20 neuroendocrine cells and modulates spontaneous action potentials and secretion (7–9). Activation of the stably expressed human D_3 dopamine receptor by dopamine inhibits spontaneous action potentials during the first application, but not upon subsequent applications (Fig. 5a). In contrast, the activation of D_3 receptors by PBZI, which does not induce tolerance and SRT, inhibits spontaneous action potentials during the first and subsequent applications (Fig. 5b). This result suggests that the modulation of neuronal firing by D_3 receptor agonists that induce tolerance is very different from those that do not induce tolerance. The latter class of agonists converts the D_3 receptor to the functional equivalent of a D_2 receptor with respect to activation of GIRK channels and modulation of action potentials.

D_3 Receptor-PBZI Pharmacophore Model Identifies a Novel Agonist that Does Not Induce Tolerance and SRT

The results in Figs. 3 and 4 showed that PD128907 induces severe tolerance and SRT; interestingly, PBZI, which does not induce tolerance or SRT shares a few core structural elements with PD128907 (Fig. 1). The stark difference in the ability of PD128907 and PBZI to induce tolerance and SRT suggested that comparative modeling studies of these compounds, docked in the D_3 receptor homology model in a dynamic mode of binding, might yield information to develop a pharmacophore model that could be used to screen for additional compounds that do not induce tolerance and SRT properties. To further understand the receptor conformations that elicited the different signaling properties induced by PD128907 and PBZI, these compounds were docked to the binding site of the D_3 receptor homology model. The docking was defined by the salt bridge interactions of the protonatable amine with Asp110, the hydrogen bond interactions with conserved serine residues in TM 5 and the aromatic interactions with residues from TM6 and TM7. The ligand-bound complexes were minimized and further refined using molecular dynamics (MD) simulations. A structural superpositioning of the refined complexes yielded a root mean square deviation (rmsd) of 3.5 Å with well-marked differences in the TM bundle as well as

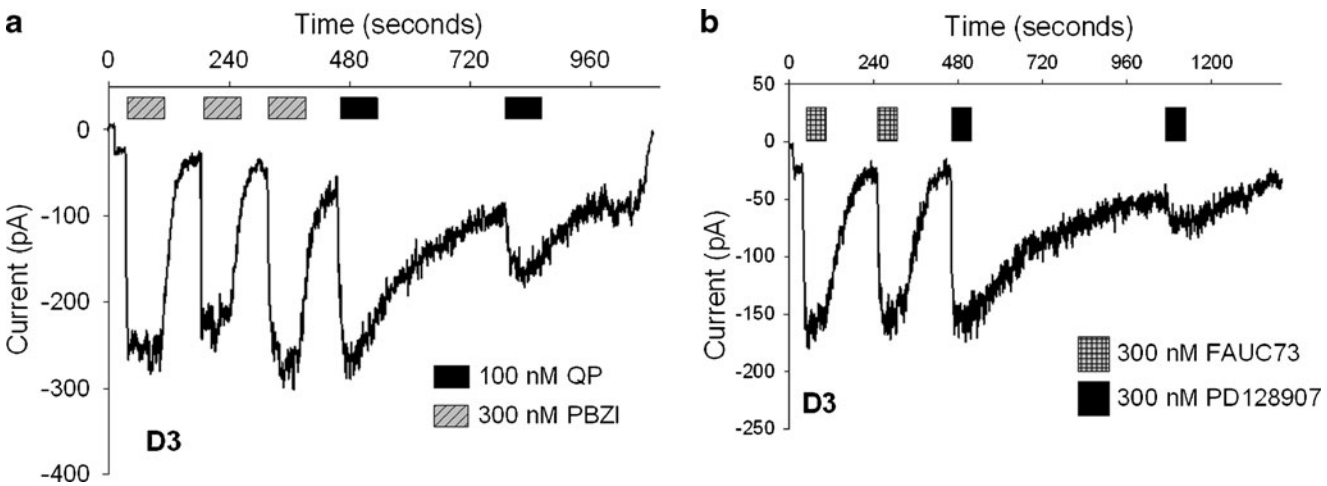

Fig. 4 D_3 receptor agonists PBZI and FAUC73 do not elicit tolerance and SRT properties. (**a**) Representative voltage clamp recording shows that 300 nM PBZI (gray hatched bar) induces GIRK currents that do not show tolerance or SRT in an AtT-20 cell stably expressing the human D_3 receptor. In contrast, in the same cell, 100 nM quinpirole (QP, black bar) elicits tolerance and SRT. (**b**) Similarly, representative voltage clamp recording shows that 300 nM FAUC73 (square crossed gray bar) induces GIRK currents that do not show D_3 receptor tolerance and SRT. In contrast, in the same cell, 300 nM PD128907 (black bar) elicits tolerance or SRT. The cells were held at −65 mV and the duration of agonist application was ~60 s.

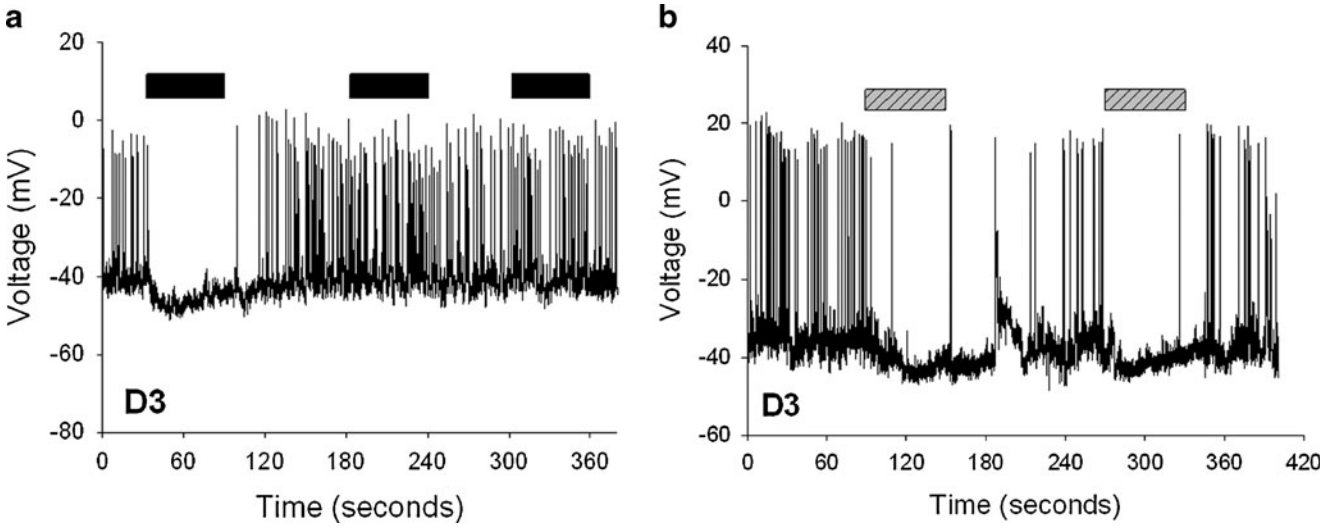

Fig. 5 Activation of D_3 receptor by dopamine and PBZI modulates neuronal firing differently. (**a**) Representative current clamp recording in an AtT-20 neuroendocrine cell stably expressing the human D_3 dopamine receptor. Activation of the D_3 receptor by 100 nM dopamine (black bar) dissolved in standard external solution with 5 mM potassium, hyperpolarizes the cell and inhibits the spontaneous action potentials during the first application but not the second or third application. (**b**) Activation of the D_3 receptor by 300 nM PBZI (gray hatched bar) dissolved in standard external solution with 5 mM potassium hyperpolarizes the cell and inhibits the spontaneous action potentials during the first and second treatment.

the loop regions (Fig. 6a), leading us to hypothesize that each of these agonists elicit a unique conformational change in the receptor as previously observed for quinpirole (12). Although PD128907 forms a conserved salt bridge with Asp110, hydrogen bonds with Ser193 on TM5 and few aromatic interactions with His349, Trp342 and Tyr373, the tetrahydropyran ring of PD128907 is more electronegative than the equivalent hexahydrobenzo group of PBZI, resulting in fewer interactions with the hydrophobic groups in TM3 as well as other aromatic residues in TM6. PBZI forms the conserved salt bridge with Asp110, hydrogen bonds with Ser192 in TM5 and has favorable cation-pi interactions with His349 and Phe345. In addition, due to the hydrophobic nature of hexahydrobenzo group, it forms favorable interactions with Val111 in TM3, Phe197 in TM5, Trp342 in TM6 and Tyr373 in TM7. Interactions of FAUC73 were similar to those of PBZI except for the loss of the hydrogen-bond interactions with Ser192, which seemed to be compensated by the gain of pi-pi interaction with His349. A three-dimensional pharmacophore incorporating the hydrophobic elements, salt bridge interaction and aromatic-pi interactions was designed to screen for additional chemical cores that could mimic the functional features of PBZI. Using this three-dimensional pharmacophore, a library of 3 million compounds was screened using the HSB method. The hits from the screen were then subjected to filtering schemes that include Lipinski's drug-like properties, pregnane xenobiotic receptor activation and, more importantly, penetration of the blood–brain barrier. The 290 hits that resulted from the filtering schemes were docked to the binding site of D_3 receptor using the GOLD program and

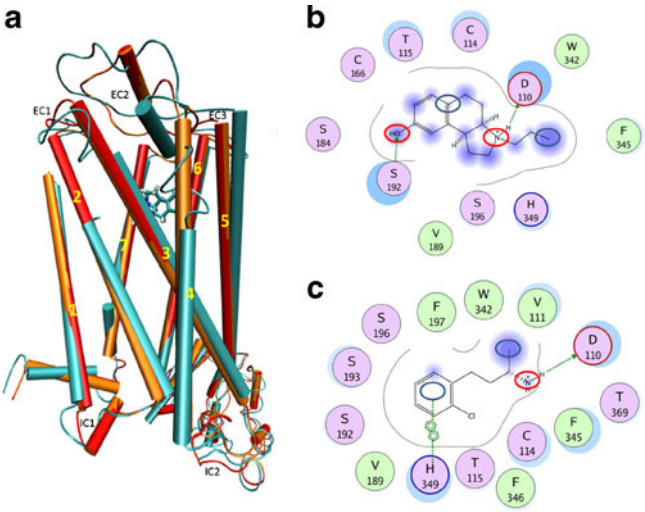

Fig. 6 The HSB method identifies residues and conformations involved in D_3 receptor tolerance and SRT properties. (**a**) Structural super positioning of D_3 receptor bound to PD128907 (cyan), PBZI (red) and ES609 (orange) is shown with the receptor represented in cartoon format. The transmembrane helices are numbered 1 through 7 and the extracellular and intracellular loops are labeled EC1-EC3 and IC1-IC3, respectively. Schematic representations of the mode of interaction of PBZI (**b**) and ES609 (**c**). The binding site residues are colored by their nature, with hydrophobic residues in green, polar residues in purple and charged residues highlighted with bold contours. Blue spheres and contours indicate matching regions between ligand and receptors. Hydrogen bonded interactions are shown by green arrows, ionic interactions in magenta lines and pi-pi interactions in green lines extending across the two six membered rings. The figures were generated using the LIGX module of the MOE program. The three-dimensional pharmacophore used to screen the molecules is overlaid on the PBZI structure with open red circles representing hydrophilic interactions, blue open circles representing hydrophobic and aromatic interactions and black dotted lines representing distance between the pharmacophore elements.

the docked complexes were scored using a variety of scoring schemes. The scoring schemes were customized to rank only those molecules that formed a salt bridge interaction with Asp110 and had favorable interactions with aromatic cluster formed by TM5, TM6 and TM7.

The 15 compounds identified by the HSB *in silico* screen were evaluated for their ability to activate D_3 receptors and induce GIRK response, tolerance, and SRT. Only compounds that demonstrated full intrinsic activity and failed to induce tolerance and SRT at D_3 receptors in the GIRK channel functional assay were chosen for further studies. Based on these stringent criteria the functional studies identified a novel D_3 receptor agonist, ES609 (4-(2-chlorophenyl)-butan-2-amine), that did not induce tolerance or SRT. Figure 7 shows representative traces and cumulative data for ES609 and suggests that, as in the case of PBZI and FAUC73, ES609 does not induce D_3 receptor tolerance or SRT properties (Fig. 7a). Control experiments showed that ES609 did not elicit GIRK currents in parental AtT-20 cells (Fig. 7b) and the currents induced in AtT-20 cells stably expressing the D_3 receptor were blocked by pretreatment with the D_2/D_3 receptor antagonist eticlopride (data not shown). Docking experiments confirmed that ES609 follows the interaction pattern of PBZI, with favorable pi-stacking interactions with His349 and salt bridge formation with Asp110 (Fig. 6b). Further refinement of the D_3 receptor-

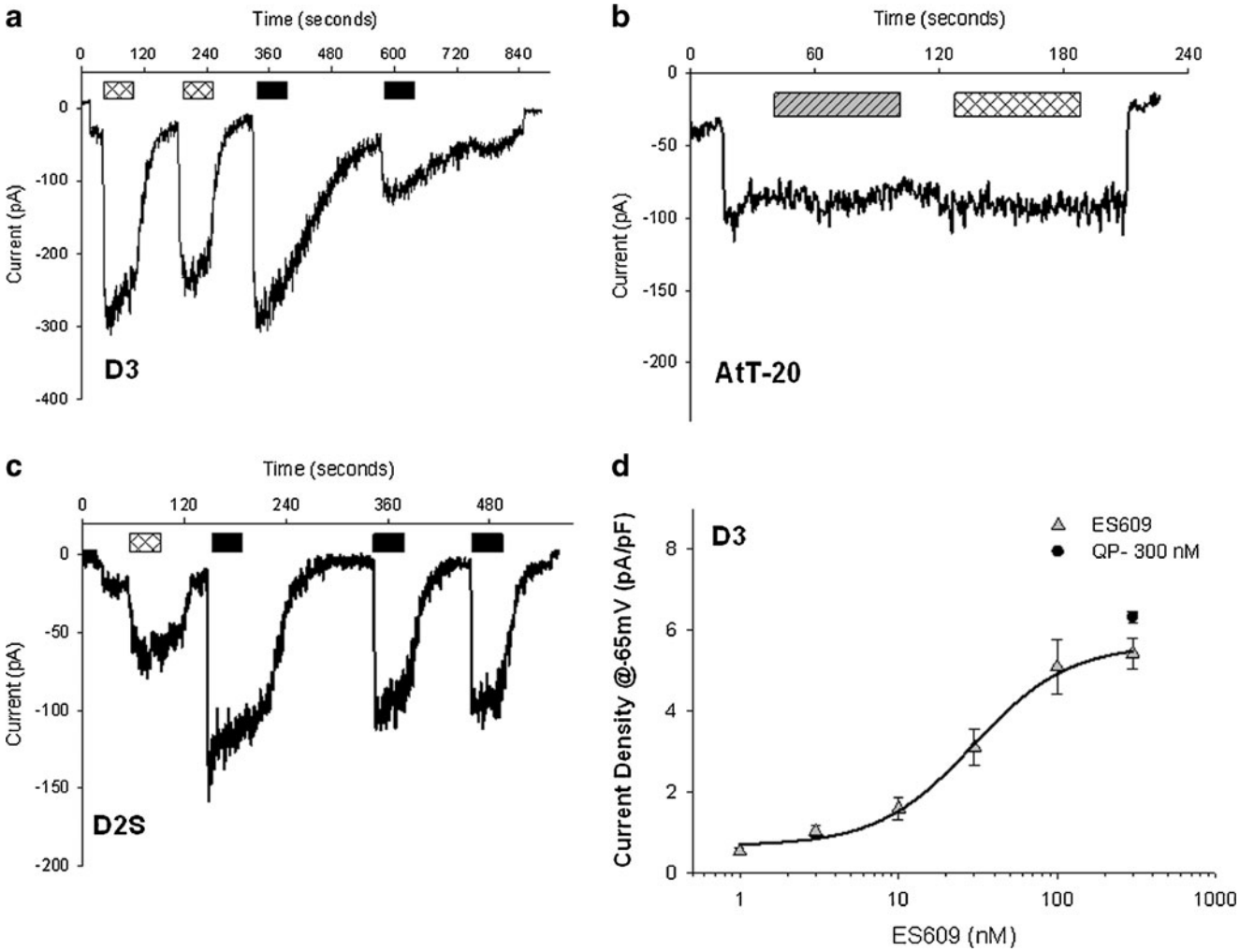

Fig. 7 Novel D_3 receptor agonist, ES609, does not induce tolerance or SRT properties. (**a**) Representative voltage clamp recording shows that 100 nM ES609 (cross hatched bar) induces GIRK currents that do not show tolerance or SRT in an AtT-20 cell stably expressing the human D_3 receptor. In contrast, in the same cell, 100 nM quinpirole (QP, black bar) elicits tolerance and SRT. (**b**) Representative voltage clamp recording shows that neither 300 nM PBZI (gray hatched bar) nor 300 nM ES609 (cross hatched bar) induce GIRK currents in parental AtT-20 cells in the absence of exogenous D_3 receptor expression. (**c**) Representative voltage clamp recording shows that 100 nM ES609 (cross hatched bar) and 100 nM quinpirole (black bar) induce GIRK currents in AtT-20 cell stably expressing the human D_{2S} receptor. The ES609-induced GIRK current is significantly less than the quinpirole-induced current in D_{2S} receptor expressing cells. The cells were held at −65 mV and the duration of agonist application was ~60 s. (**d**) Cumulative dose response of ES609-induced GIRK response in AtT-20 cells stably expressing the human D_3 receptor. The black filled circle is the GIRK response elicited by a high dose of quinpirole (QP, 300 nM) and shows that ES609 has full intrinsic activity at the D_3 receptor-GIRK channel pathway. Error bars represent ± SEM. The GIRK currents were divided by cell capacitance (pF) to normalize for cell size. The data points were fit with a four-parameter Hill equation.

Table I PBZI Induced Inhibition of Adenylate Cyclase and Activation of GIRK Channels in AtT-20 Cells Stably Expressing the Individual Dopamine Receptor Subtypes

D2-like dopamine receptor	Adenylate cyclase inhibition EC_{50} (nM)	Adenylate cyclase inhibition (%)			GIRK channel activation EC_{50} (nM)	GIRK channel activation (pA/pF)		
		300 nM QP	300 nM PBZI	Ratio PBZI/QP		300 nM QP	300 nM PBZI	Ratio PBZI/QP
D_{2S}	>150	64.4 ± 2.3	32.9 ± 1.8[a]	0.51	53 ± 19.8	11.7 ± 0.3	5.6 ± 1.4[c]	0.48
D_{2L}	67 ± 15	74.1 ± 0.3	61.4 ± 1.1	0.83	ND	12.8 ± 1.3	10.6 ± 0.9	0.83
D_3	35 ± 2.8	55.9 ± 1.7	54.2 ± 1.7	0.97	29 ± 16.1	6.3 ± 0.14	8.1 ± 1.1	1.3
$D_{4.2}$	No response	76.8 ± 0.7	0[b]	0	ND	7.6 ± 1.1	2.7 ± 0.9[d]	0.35

[a, b] $P < 0.05$, statistically significant, Student's t-test comparing the percent inhibition of 10 μM forskolin-induced cAMP levels elicited by 300 nM PBZI and 300 nM quinpirole in the adenylate cyclase assay. [c, d] $P < 0.05$, statistically significant, Student's t-test comparing the agonist-activated current densities elicited by 300 nM PBZI and 300 nM quinpirole in the GIRK channel assay. ND- not determined; a full dose–response experiment to determine EC_{50} was not performed; data was obtained for a single concentration (300 nM) of PBZI. ± Standard Error of Mean.

ES609 complex using MD simulation studies showed that ES609 elicits a conformation similar to that of PBZI. ES609-bound D_3 receptor structure superpositioned on to the PBZI-bound D_3 receptor structure with an RMSD of 1.2Å (Fig. 6a); in contrast, ES609-bound D_3 receptor structure superpositioned on to the dopamine-bound D_3 receptor structure with an RMSD of 3.4Å. Taken together, the results suggest that while ES609 has the same core structure as that of dopamine (Fig. 1), its interaction pattern and the conformational change it elicits in the D_3 receptor are similar to those of PBZI (Fig. 6c). These differences between dopamine and PBZI/ES609 might contribute to the inability of the latter agonists to elicit D3 receptor tolerance and SRT properties.

Functional Characterization of PBZI and ES609

To compare the functional effects of the new class of D_3 receptor agonists, we tested PBZI (Table I) and ES609 (Table II) on AtT-20 cells stably expressing human D_3, D_{2S}, D_{2L}, or $D_{4.2}$. Functional efficacy was determined by assessing the ability of PBZI and ES609 to inhibit adenylate cyclase or activate GIRK channels coupled to these "D2-like" dopamine receptors. The EC_{50} values of PBZI and ES609 for inhibiting adenylate cyclase and activating GIRK channels are in the range of 0.2 nM to 30 nM for D_3 receptors. We compared the functional responses elicited by PBZI and ES609 to those elicited by quinpirole, an agonist that at 300 nM has full intrinsic activity at D_{2S}, D_{2L}, D_3, and D_4 dopamine receptors in these two functional assays. Comparing PBZI- and ES609-elicited functional response to the functional response elicited by a high concentration of the full agonist, quinpirole, allowed us to determine the relative intrinsic activity of PBZI and ES609 in cell lines expressing the different D2-like dopamine receptors. The results show that PBZI and ES609 have full intrinsic activity at D_3 receptors in both the adenylate cyclase and GIRK channel assays. Both PBZI and ES609 are partial agonists at the D_{2S} dopamine receptor (Table I and II; Fig. 8a). At D_{2L} dopamine receptors, PBZI has full intrinsic activity in both assays (Table I; Fig. 8b); in contrast, ES609 does not elicit any response in the adenylate cyclase assay and is a partial agonist in the GIRK channel assay (Table II; Fig. 8b). We have previously shown that the expression level of D_{2S} (854 ± 20 fmol/mg) and D_{2L} (1032 ± 51 fmol/mg) receptors in the stable AtT20 cell lines are

Table II ES609 Induced Inhibition of Adenylate Cyclase and Activation of GIRK Channels in AtT-20 Cells Stably Expressing the Individual Dopamine Receptor Subtypes

D2-like dopamine receptor	Adenylate cyclase inhibition EC_{50} (nM)	Adenylate cyclase inhibition (%)			GIRK channel activation EC_{50} (nM)	GIRK channel activation (pA/pF)		
		300 nM QP	300 nM ES609	Ratio ES609/QP		300 nM QP	300 nM ES609	Ratio ES609/QP
D_{2S}	2.4 ± 0.2	66.4 ± 2.8	19.5 ± 1.6[a]	0.29	ND	11.7 ± 0.3	3.5 ± 0.8[d]	0.30
D_{2L}	No response	76.1 ± 0.8	0[b]	0	ND	12.8 ± 1.3	4.1 ± 0.6[e]	0.32
D_3	0.15 ± 0.06	58.2 ± 7.7	41.3 ± 3.3	0.71	30 ± 7.7	6.3 ± 0.14	5.4 ± 0.4	0.86
$D_{4.2}$	0.82 ± 0.3	78.8 ± 0.4	47.3 ± 3.7[c]	0.60	No response	7.6 ± 1.1	0[f]	0

[a, b, c] $P < 0.05$, statistically significant, Student's t-test comparing the percent inhibition of 10 μM forskolin-induced cAMP levels elicited by 300 nM ES609 and 300 nM quinpirole in the adenylate cyclase assay. [d, e, f] $P < 0.05$, statistically significant, Student's t-test comparing the agonist-activated current densities elicited by 300 nM ES609 and 300 nM quinpirole in the GIRK channel assay. ND- not determined; a full dose–response experiment to determine EC_{50} was not performed; data was obtained for a single concentration (300 nM) of ES609. ± Standard Error of Mean.

comparable (10). At $D_{4.2}$ dopamine receptors, PBZI elicits no response (Table I) and ES609 is a partial agonist in the adenylate cyclase assay (Fig. 9a). In the GIRK channel assay, PBZI is a partial agonist at $D_{4.2}$ receptors, whereas ES609 elicits no response (Fig. 9b). Together these results suggest that both PBZI and ES609 have full intrinsic activity at D_3 receptor and exhibits partial agonism at D_{2S} dopamine receptors in both the adenylate cyclase and GIRK channel assays. Whereas PBZI exhibits functional selectivity at $D_{4.2}$, ES609 is functionally selective at D_{2L} and $D_{4.2}$ dopamine receptors.

DISCUSSION

D_3 dopamine receptor tolerance and SRT properties were first observed in primary cultures of substantia nigra pars compacta neurons treated with the D_2/D_3 receptor agonist quinpirole (28). These properties were also observed in human D_3 receptors expressed in *Xenopus* oocytes (6). We have previously characterized human D_3 receptor tolerance and SRT properties in AtT-20 and CHO cells and identified the key residues and domains that determine these properties (4,10,11). In this paper we demonstrate that the D_3 receptor tolerance and SRT properties are ligand dependent and we identify a new class of atypical D_3 receptor agonists that do not induce these properties. Currently, this novel class of D_3 receptor agonist has three members, including two previously known compounds and one novel compound. In a functional screen, we initially identified PBZI, a water-soluble compound that is structurally similar to PD128907 but does not induce tolerance or SRT. Previous binding studies have shown that for D2-like receptors, PBZI has a Ki of 27 nM for D_3, 1800 nM for D_{2S} and 280 nM for $D_{4.2}$ (25). Binding at D1-like receptors and a panel of other neurotransmitter receptors, ion channels and transporters was negligible (25). Functionally, a previous *in vitro* study showed that PBZI is a partial agonist at D_{2S} receptors (25). This finding is consistent with the result from our functional studies showing that PBZI is a full agonist at D_3 receptors and a partial agonist at the D_{2S} dopamine receptors (Table I). *In vivo*, animals administered PBZI, show specific increases in *c-fos* expression in the medial prefrontal cortex and in the shell region of nucleus accumbens, regions with high D_3 receptor expression (25). The effect of PBZI on D_{2L} receptors had not been previously determined. Our results show that, PBZI is a full agonist at the D_{2L} dopamine receptor (Table I). More importantly, the differential efficacy of PBZI at D_{2S} and D_{2L} receptor is intriguing and, to our knowledge, this agonist represents the first that has been shown to pharmacologically distinguish the function of the two D_2 receptor splice isoforms (29). D_{2S} and D_{2L} receptors are located and modulate dopaminergic neurotransmission pre- and post-synaptically, respectively (30,31). Given the differential efficacy at D_{2S} and D_{2L} receptors, PBZI would be predicted to have primarily postsynaptic effects. This is supported by previous *in vivo* studies in which PBZI-induced contralateral rotations in rats with 6-OHDA lesions were not blocked by D_1 or D_3 receptor-selective antagonists (26).

The classical D2-like receptor agonist, PD128907, has a relatively high affinity for D_3 receptor and is widely used both *in vitro* and *in vivo* (32). Our study shows that PD128907 induces severe tolerance and SRT at the D_3 receptor (Fig. 3). Interestingly, the chemical structure of PD128907 is similar to PBZI (Fig. 1). Although PD128907 and PBZI share a similar core structure and function as full agonists at the D_3 receptor, they have dramatically different effects on

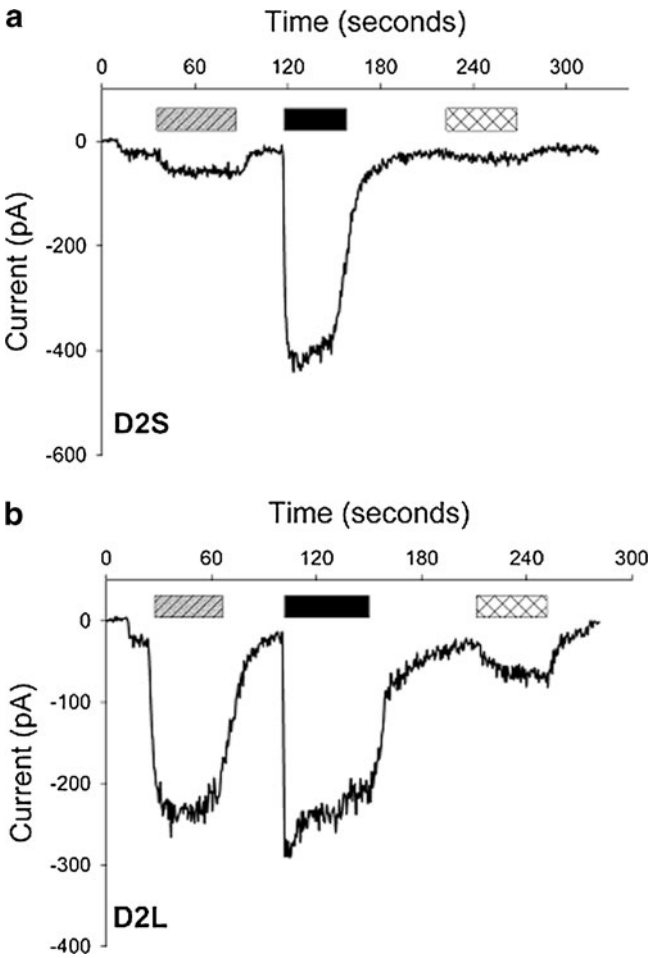

Fig. 8 PBZI exhibits different intrinsic efficacy at D_{2S} and D_{2L} dopamine receptors. Representative voltage clamp recordings in AtT-20 cells stably expressing the human D_{2S} (**a**) and human D_{2L} (**b**) dopamine receptors. The representative results shows that 300 nM PBZI (gray hatched bar), quinpirole (black bar) and ES609 (cross hatched bar) induce GIRK currents of different magnitude in AtT-20 cells stably expressing the human D_{2S} (**a**) and D_{2L} (**b**) dopamine receptor. Specifically, compared to full agonist quinpirole (black bar), PBZI (gray hatched bar) elicits a very small response in D2S-expressing cell (**a**) while eliciting a response equivalent to quinpirole in D2L-expressing cell (**b**). The cells were held at −65 mV and the duration of agonist application is indicated by the length of the bars.

the tolerance and SRT properties (Figs. 3 and 4). Results from the modeling studies suggest that the functional differences between PBZI and PD128907 are due to the different conformation these agonists induce in the D_3 receptor. The majority of these conformational changes are confined to the regions closest to the binding site and extracellular loop (EC) 2 loop region. Comparison of the PBZI- and PD128907-bound structures suggests that the maximum shift occurs in TM4 which is coupled with large movements of EC2. In addition, conformational changes are observed in intracellular loop (IC) 2 which we have previously shown to be important for mediating the tolerance property (12). Other significant conformational changes include a downward shift along the length of the TM6 helix and an unwinding of the first turn of the TM3 helix in the PD128907-bound form. The crystal structure of dopamine D_3 receptor in complex with a selective *antagonist* was published recently (14). Comparison of our agonist-bound model with that of the published crystal structure showed minimal deviations within the TM bundles, the exception being TM3, TM5 and TM6 where the RMSD varied between 2 and 3 Å. The loop regions connecting TM3, TM4, TM5 and TM6 showed deviations greater than 3Å. The IC2 in the agonist-bound conformation did not form a helix as reported in the antagonist-bound form (14). The observed differences between the agonist and antagonist forms are in agreement with the previous studies reported in the literature for other GPCRs (33–35).

In this study, by carefully monitoring the conformational effects produced by the binding of PBZI and PD128907 in computational models, we identified a novel atypical D_3 receptor agonist, ES609, which does not induce the D_3 receptor tolerance and SRT properties and exhibits functional selectivity at D_{2L} and $D_{4.2}$ dopamine receptors. We are currently using the HSB method to identify additional atypical D_3 receptor agonists. ES609 was identified by screening a 3 million compound library for small molecules that could mimic the pharmacophore features of PBZI. Our hypothesis was to increase the strength of the pi-pi interactions with the aromatic core by introducing electron withdrawing groups on the ligand. Thus the halogen group at the ortho position in ES609 was highly suitable to the design, along with the added hydrophobicity proximal to the protonatable amine (Fig. 6c). The latter strengthened the interactions with hydrophobic groups on TM3 similar to the interactions of FAUC73 with residues in TM3. It has been recently shown that His349 may play a major role in promoting ligand biased signaling in D_{2L} receptor (36). These results are consistent with our findings that strengthening the pi-pi interactions with His349 and introducing additional hydrophobic moieties that can form favorable hydrophobic interactions with TM3 and TM6 may contribute favorably to the unique conformational changes that could lead to the inability to induce tolerance and SRT by PBZI, FAUC73 and ES609.

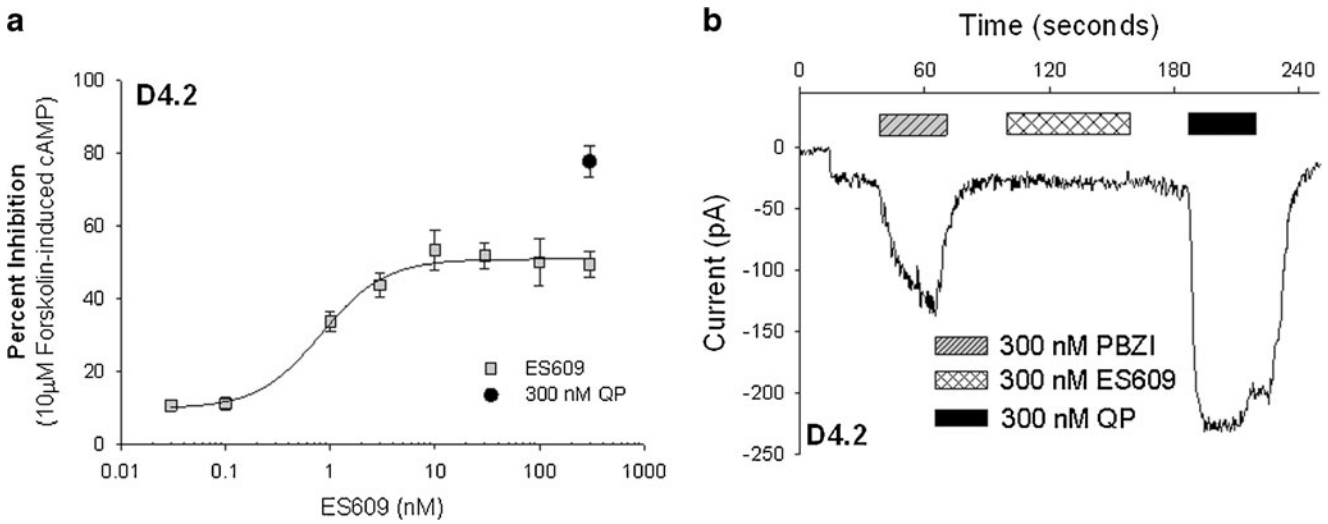

Fig. 9 ES609 exhibits functional selectivity at $D_{4.2}$ dopamine receptors. (**a**) Dose-dependent inhibition of 10 μM forskolin-induced cAMP levels by ES609 in AtT-20 cells stably expressing the human $D_{4.2}$ dopamine receptors. Cells were treated with 10 μM forskolin and 300 μM IBMX and different concentrations of ES609 for 30 min at 37 °C. In each experiment control cells were also treated with 300 nM quinpirole (QP) and forskolin-IBMX (dark circles). Cellular cAMP levels were measured using the BioTrak immunoassay kit from GE Healthcare. The cAMP levels in each sample were normalized to the total protein concentration to minimize well-to-well variability in cell density. Percent inhibition values for each ES609 or quinpirole concentration were determined by comparing the cAMP levels to control cells treated with just forskolin and IBMX. The cAMP measurement assays were performed in triplicate. (**b**) Representative voltage clamp recording shows that 300 nM PBZI (gray hatched bar), ES609 (cross hatched bar) and quinpirole (black bar) induce GIRK currents of different magnitude in AtT-20 cells stably expressing the human $D_{4.2}$ dopamine receptor. The cells were held at −65 mV and the duration of agonist application is indicated by the length of the bars.

Functionally, ES609 and PBZI have similar efficacy for activating D_3 receptor coupled signal transduction pathways. In contrast to PBZI, however, ES609 is either a partial agonist or elicits no response at other D2-like receptors (D_{2S}, D_{2L} and $D_{4.2}$) when tested in two different signaling pathways. The selectivity exhibited by ES609 for D_3 receptors suggests that its structure could serve as a template for designing future selective D_3 receptor agonists. The potency of ES609, defined by it EC_{50}, is similar to other D2-like dopamine receptor agonists in the two signaling pathways that we studied. Furthermore, its small molecular weight and water solubility makes it ideally suited for *in vivo* studies. Given that PBZI and ES609 have similar signaling properties *in vitro*, they are expected to have a similar effect *in vivo*.

CONCLUSION

Functional selectivity is defined as the ability of different ligands to elicit varying responses in different signal transduction pathways coupled to the same receptor (37–40). The ability of ligands to activate different pathways coupled to the same receptor to different degrees results from the different conformations that the ligand engenders in the receptor (39). For D2-like dopamine receptors, dihydrexidine and its analogs elicit functional selectivity at D_2 receptors (41,42). To our knowledge, functionally-selective agonists for D_3 and D_4 dopamine receptors have not been previously described. Our results suggest that PBZI exhibits functional selectivity at $D_{4.2}$ (Table I) and that ES609 exhibits functional selectivity at D_{2L} and $D_{4.2}$ (Table II). Both agonists exhibit full intrinsic efficacy at the D_3 receptor-GIRK channel and at adenylate cyclase signaling pathways. More interestingly, PBZI, ES609 and FAUC73 do not induce the D_3 receptor tolerance and SRT properties that we have previously shown are determined by distinct conformations states (12). The newly identified D_3 receptor agonists most likely induce a different D_3 receptor conformation, which while retaining the ability to couple to downstream signal transduction pathways fails to induce the D_3 receptor tolerance and SRT properties. D_3 receptor structural components described in our previous studies (4,11) are likely to be involved. Indeed, we recently showed that the D_3 receptor conformation elicited by PBZI is distinct from that elicited by tolerance-inducing quinpirole but similar to the mutant C147K D_3 receptor that does not show tolerance (12). This suggests that the inability to induce tolerance and SRT is associated with a distinct yet stable D_3 receptor conformation.

The expression of D_3 dopamine receptor is altered under many pathological conditions and following chronic drug treatment. Ectopic expression or alterations in the D_3 receptor tolerance and SRT properties could underlie the pathology of various disorders. In Parkinson's disease, levodopa-induced dyskinesias are associated with a specific up regulation of D_3 receptor expression in putamen and globus pallidus internal segment, regions that normally express the D_2 receptor (43–45). In rodent models, the behavioral sensitization associated with levodopa treatment is mediated by upregulated D_3 receptors (44,46). We have proposed that the alteration of the ratio of D_3/D_2 receptor expression and the ectopic expression of D_3 receptor tolerance and SRT properties in the striatum of animals with levodopa-induced dyskinesia could contribute to the dyskinetic behavior (4). We are currently determining the ability of atypical D_3 receptor agonists described in this paper to improve levodopa-induced dyskinesia in animal models of Parkinson's disease.

ACKNOWLEDGMENTS & DISCLOSURES

This work was supported by the UMDNJ and the F. M. Kirby Foundations to EVK and American Heart Association–scientist development grant and Faculty start-up funds from Drexel University College of Medicine to SK. We thank Diana Winters (Academic Publishing Services, Drexel University College of Medicine) for proof-reading the manuscript. The authors declare no conflicts of interest.

REFERENCES

1. Ahlgren-Beckendorf JA, Levant B. Signaling mechanisms of the D_3 dopamine receptor. J Recept Signal Transduct Res. 2004;24 (3):117–30.
2. Robinson SW, Caron MG. Selective inhibition of adenylate cyclase type V by the dopamine D3 receptor. Mol Pharmacol. 1997;52: 508–14.
3. Cussac D, Newman-Tancredi A, Pasteau V, Millan MJ. Human dopamine D(3) receptors mediate mitogen-activated protein kinase activation via a phosphatidylinositol 3-kinase and an atypical protein kinase C-dependent mechanism. Mol Pharmacol. 1999;56 (5):1025–30.
4. Westrich L, Kuzhikandathil EV. The tolerance property of human D3 dopamine receptor is determined by specific amino acid residues in the second cytoplasmic loop. Biochimica et Biophysica Acta- MCR. 2007;1773:1747–58.
5. Seabrook GR, Kemp JA, Freedman SB, Patel S, Sinclair HA, McAllister G. Functional expression of human D3 dopamine receptors in differentiated neuroblastoma X glioma NG108-15 cells. Br J Pharmacol. 1994;111:391–3.
6. Werner P, Hussy N, Buell G, Jones KA, North RA. D2, D3, and D4 dopamine receptors couple to G protein-regulated potassium channels in Xenopus oocytes. Mol Pharmacol. 1996;49:656–61.
7. Kuzhikandathil EV, Yu W, Oxford GS. Human dopamine D3 and D2L receptors couple to inward rectifier potassium channels in mammalian cell lines. Mol Cell Neurosci. 1998;12:390–402.
8. Kuzhikandathil EV, Oxford GS. Activation of human D3 dopamine receptor inhibits P/Q-type calcium channels and secretory activity in AtT-20 cells. J Neurosci. 1999;19(5):1698–707.
9. Kuzhikandathil EV, Oxford GS. Dominant-negative mutants identify a role for GIRK channels in D3 dopamine receptor-

mediated regulation of spontaneous secretion activity. J Gen Physiol. 2000;115:697–706.
10. Kuzhikandathil EV, Bartoszyk GD. The novel antidyskinetic drug sarizotan elicits different functional responses at human D2-like dopamine receptors. Neuropharmacol. 2006;51:873–84.
11. Kuzhikandathil EV, Westrich L, Bakhos S, Pasuit J. Identification and characterization of novel properties of the human D3 dopamine receptor. Mol Cell Neurosci. 2004;26:144–55.
12. Westrich L, Gil-Mast S, Kortagere S, Kuzhikandathil EV. Development of tolerance in D3 dopamine receptor signaling is accompanied by distinct changes in receptor conformation. Biochem Pharmacol. 2010;79:897–907.
13. Kortagere S, Welsh WJ. Development and application of hybrid structure based method for efficient screening of ligands binding to G-protein coupled receptors. J Comput Aided Mol Des. 2006;20 (12):789–802.
14. Chien EY, Liu W, Zhao Q, Katritch V, Han GW, Hanson MA, *et al.* Structure of the human dopamine D_3 receptor in complex with a D2/D3 selective antagonist. Science. 2010;330(6007):1091–115.
15. Cherezov V, Rosenbaum DM, Hanson MA, Rasmussen SG, Thian FS, Kobilka TS, *et al.* High-resolution crystal structure of an engineered human beta2-adrenergic G protein-coupled receptor. Science. 2007;318(5854):1258–65.
16. Sali A, Blundell TL. Comparative protein modelling by satisfaction of spatial restraints. J Mol Biol. 1993;234(3):779–815.
17. Kortagere S, Cheng SY, Antonio T, Zhen J, Reith ME, Dutta AK. Interaction of novel hybrid compounds with the D3 dopamine receptor: Site-directed mutagenesis and homology modeling studies. Biochem Pharmacol. 2011;81(1):157–63.
18. Jones G, Willett P, Glen RC. Molecular recognition of receptor sites using a genetic algorithm with a description of desolvation. J Mol Biol. 1995;245(1):43–53.
19. Eldridge MD, Murray CW, Auton TR, Paolini GV, Mee RP. Empirical scoring functions: I. The development of a fast empirical scoring function to estimate the binding affinity of ligands in receptor complexes. J Comput Aided Mol Des. 1997;11(5):425–45.
20. Kevin J, Bowers EC, Xu H, Dror RO, Eastwood MP, Gregersen BA, *et al.* Scalable Algorithms for Molecular Dynamics Simulations on Commodity Clusters. Proceedings of the ACM/IEEE Conference on Supercomputing (SC06), New York, NY, IEEE; 2006.
21. Lipinski CA, Lombardo F, Dominy BW, Feeney PJ. Experimental and computational approaches to estimate solubility and permeability in drug discovery and development settings. Adv Drug Deliv Rev. 2001;46(1–3):3–26.
22. Kortagere S, Chekmarev D, Welsh WJ, Ekins S. New predictive models for blood–brain barrier permeability of drug-like molecules. Pharm Res. 2008;25(8):1836–45.
23. Kortagere S, Chekmarev D, Welsh WJ, Ekins S. Hybrid scoring and classification approaches to predict human pregnane X receptor activators. Pharm Res. 2009;26(4):1001–11.
24. Chekmarev DS, Kholodovych V, Balakin KV, Ivanenkov Y, Ekins S, Welsh WJ. Shape signatures: new descriptors for predicting cardiotoxicity in silico. Chem ResToxicol. 2008;21(6):1304–14.
25. Scheideler MA, Martin J, Hohlweg R, Rasmussen JS, Naerum L, Ludvigsen TS, *et al.* The preferential dopamine D3 receptor agonist cis-8-OH-PBZI induces limbic Fos expression in rat brain. Eur J Pharmacol. 1997;339(2–3):261–70.
26. Fink-Jensen A, Nielsen EB, Hansen L, Scheideler MA. Behavioral and neurochemical effects of the preferential dopamine D3 receptor agonist cis-8-OH-PBZI. Eur J Pharmacol. 1998;342(2–3):153–61.
27. Malik P, Andersen MB, Peacock L. The effects of dopamine D3 agonists and antagonists in a nonhuman primate model of tardive dyskinesia. Pharmacol Biochem Behav. 2004;78(4):805–10.
28. Kim KM, Nakajima Y, Nakajima S. G protein-coupled inward rectifier modulated by dopamine agonists in cultured substantia nigra neurons. Neurosci. 1995;69:1145–58.
29. Centonze D, Gubellini P, Usiello A, Rossi S, Tscherter A, Bracci E, *et al.* Differential contribution of dopamine D2S and D2L receptors in the modulation of glutamate and GABA transmission in the striatum. Neuroscience. 2004;129(1):157–66.
30. Khan ZU, Mrzljak L, Gutierrez A, de la Calle A, Goldman-Rakic PS. Prominence of the dopamine D2 short isoform in dopaminergic pathways. Proc Natl Acad Sci (USA). 1998;95(13):7731–6.
31. Lindgren N, Usiello A, Goiny M, Haycock J, Erbs E, Greengard P, *et al.* Distinct roles of dopamine D2L and D2S receptor isoforms in the regulation of protein phosphorylation at presynaptic and postsynaptic sites. Proc Natl Acad Sci (USA). 2003;100(7):4305–9.
32. Pugsley TA, Davis MD, Akunne HC, MacKenzie RG, Shih YH, Damsma G, *et al.* Neurochemical and functional characterization of the preferentially selective dopamine D3 agonist PD 128907. J Pharmacol Exp Ther. 1995;275(3):1355–66.
33. Rasmussen SGF, Choi H-J, Fung JJ, Pardon E, Casarosa P, Chae PS, *et al.* Structure of a nanobody-stabilized active state of the [beta]2 adrenoceptor. Nature. 2011;469:175–80.
34. Rosenbaum DM, Zhang C, Lyons JA, Holl R, Aragao D, Arlow DH, *et al.* Structure and function of an irreversible agonist-[beta]2 adrenoceptor complex. Nature. 2011;469:236–40.
35. Warne T, Moukhametzianov R, Baker JG, Nehme R, Edwards PC, Leslie AGW, *et al.* The structural basis for agonist and partial agonist action on a [beta]1-adrenergic receptor. Nature. 2011;469: 241–4.
36. Tschammer N, Bollinger S, Kenakin T, Gmeiner P. Histidine 6.55 is a major determinant of ligand-biased signaling in dopamine D2L receptor. Mol Pharmacol. 2011;79(3):575–85.
37. Kenakin T. Ligand-selective receptor conformations revisited: the promise and the problem. Trends Pharmacol Sci. 2003;24 (7):346–54.
38. Mailman RB. GPCR functional selectivity has therapeutic impact. Trends Pharmacol Sci. 2007;28(8):390–6.
39. Urban JD, Clarke WP, von Zastrow M, Nichols DE, Kobilka B, Weinstein H, *et al.* Functional selectivity and classical concepts of quantitative pharmacology. J Pharmacol Exp Ther. 2007;320(1):1–13.
40. Kenakin T, Miller LJ. Seven transmembrane receptors as shapeshifting proteins: the impact of allosteric modulation and functional selectivity on new drug discovery. Pharmacol Rev. 2010;62(2):265–304.
41. Kilts JD, Connery HS, Arrington EG, Lewis MM, Lawler CP, Oxford GS, *et al.* Functional selectivity of dopamine receptor agonists. II. Actions of dihydrexidine in D2L receptor-transfected MN9D cells and pituitary lactotrophs. J Pharmacol Exp Ther. 2002;301(3):1179–89.
42. Mottola DM, Kilts JD, Lewis MM, Connery HS, Walker QD, Jones SR, *et al.* Functional selectivity of dopamine receptor agonists. I. Selective activation of postsynaptic dopamine D2 receptors linked to adenylate cyclase. J Pharmacol Exp Ther. 2002;301(3):1166–78.
43. Bezard E, Ferry S, Mach U, Stark H, Leriche L, Boraud T, *et al.* Attenuation of levodopa-induced dyskinesia by normalizing dopamine D_3 receptor function. Nat Med. 2003;9(6):762–7.
44. Bordet R, Ridray S, Carboni S, Diaz J, Sokoloff P, Schwartz JC. Induction of dopamine D3 receptor expression as a mechanism of behavioral sensitization to levodopa. Proc Natl Acad Sci (USA). 1997;94(7):3363–7.
45. Guigoni C, Aubert I, Li Q, Gurevich VV, Benovic JL, Ferry S, *et al.* Pathogenesis of levodopa-induced dyskinesia: focus on D1 and D3 dopamine receptors. Parkinsonism Related Disorders. 2005;11 Suppl 1:S25–29.
46. Guillin O, Diaz J, Carroll P, Griffon N, Schwartz JC, Sokoloff P. BDNF controls dopamine D3 receptor expression and triggers behavioural sensitization. Nature. 2001;411(6833):86–9.
47. Jorgensen WL, Maxwell DS, Tirado-Rives J. Development and testing of the OPLS all-atom force field on conformational energetics and properties of organic liquids. J Am Chem Soc. 1996;118 (45):11225–36.